A&A 395, 853–862 (2002)
DOI: 10.1051/0004-6361:20021300

Astronomy & Astrophysics

The 2-D structure of dusty disks around Herbig Ae/Be stars

I. Models with grey opacities

C. P. Dullemond

Max Planck Institut für Astrophysik, PO Box 1317, 85741 Garching, Germany
e-mail: dullemon@mpa-garching.mpg.de

Receved 19 July 2002 / Accepted 16 August 2002

Abstract. In this paper the two-dimensional structure of protoplanetary disks around Herbig Ae/Be stars is studied. This is done by constructing a self-consistent model based on 2-D radiative transfer coupled to the equation of vertical hydrostatics. As a simplifying assumption a grey opacity is used. It is found that the disk can adopt four different structures, dependent on the surface density distribution $\Sigma(R)$ as a function of radius, i.e. on radial- and vertical optical depth of the disk. For the case of high to intermediate vertical optical depth, the temperature and density structures are in agreement with the simple "disk with inner hole" model of Dullemond et al. (2001, henceforth DDN01). At large radii the disk adopts a flaring shape as expected, and near the dust destruction radius (located at about 0.5 AU for most Herbig Ae stars) the disk is superheated and puffs up. The region directly behind this "puffed-up inner dust wall" is shadowed, as predicted by DDN01. For the case of intermediate to low vertical optical depth, but still high radial optical depth, the 2-D models show that the shadow can cover the entire disk. For such competely self-shadowed disks the inner rim emission in the near infrared constitutes the dominant part of the SED, since the flaring component in the mid- and far infrared is suppressed by the self-shadowing effect. When the disk is optically thin even in radial direction, it becomes unshadowed again because the inner rim can no longer block the stellar light. Such disks have relatively weak infrared excess compared to the stellar flux. Finally, for disks that flare at intermediate radii, but become too optically thin at large radii, the outer parts once again become shadowed. But this time the shadowing is caused by the flaring part of the disk, instead of the inner rim. The disk then consists of a bright inner rim, a shadow, a flaring part and finally a (dim) shadowed outer part. Different observational methods of determining the size of the disk (e.g. from the SED, from continuum mapping or from CO mapping) may yield different results.

Key words. accretion, accretion disks – stars: circumstellar matter – stars: formation – stars: pre-main-sequence – infrared: stars

1. Introduction

Herbig Ae/Be stars are widely regarded as the intermediate mass counterparts of the lower mass T Tauri stars (e.g. Strom et al. 1972; Palla & Stahler 1993; v.d. Ancker et al. 1998). But, while there is little doubt that the infrared excess of classical T Tauri stars originates in a protoplanetary disk, the case for Herbig Ae/Be stars is not so clear. On large scales the disk-like nature of the circumstellar matter around Herbig Ae/Be stars is by now well established. Millimeter CO and continuum maps (Mannings & Sargent 1997), submm position-velocity maps (Qi 2001) and imaging at visible and near-infrared wavelengths (Grady et al. 1999; Augereau 2001) clearly show rotating flattened structures at scales of hundreds of AU. But on scales of tens of AU and smaller there seems to be conflicting evidence, with some authors arguing for a more or less spherical geometry (di Francesco et al. 1994; Pezzuto et al. 1997; Miroshnichenko et al. 1997, 1999; Millan-Gabet et al. 2001) and others favoring the disk-like picture (Vink et al. 2003; Grinin & Rostopchina 1996; Natta et al. 2001; Tuthill et al. 2001).

Unfortunately, for some time disk models have failed to explain the SEDs of Herbig Ae/Be stars, and were consequently rejected by many. In particular the conspicuous bump around 3 microns in the SEDs of Herbig Ae/Be stars remained a mystery. Standard disk models such as those of Chiang & Goldreich (1997, henceforth CG97), and D'Alessio et al. (1998, 1999) failed to explain this striking feature. Several explanations were suggested, ranging from FeO dust at 800 K (v.d. Ancker et al. 2000) to accretion disks that are actively dissipating only beyond a certain radius (Hillenbrand et al. 1992). None of these explanations were quite satisfactory. Recently, it was recognized by Natta et al. (2001) that this 3 micron bump may well originate from the inner rim of the dusty part of the disk. Since dust evaporates above about 1500 K, the inner parts of the disk are free of dust. These gaseous inner parts have a much lower optical depth, and can even be entirely optically thin, depending on the gas surface density. At the dust

evaporation radius the dust forms a wall of 1500 K that is directly irradiated by the central star. This produces an extra component in the spectrum that was not considered by the existing models of flaring disks.

Dullemond et al. (2001, henceforth DDN01) adapted the CG97 model to self-consistently include this inner rim, and showed that the SEDs of Herbig Ae/Be stars can be naturally explained in this way. In a recent paper (Dominik et al. 2002) the sample of 14 Herbig Ae/Be stars of Meeus et al. (2001) was analyzed in the context of this model, and it was found that the SEDs of most stars were indeed consistent with the DDN01 picture.

According to this model, the inner rim of the flaring disk is much hotter than an ordinary flaring disk model would predict at that radius. This is because the inner rim is irradiated frontally rather than at a grazing angle. As a consequence, the inner rim is puffed up and casts a shadow over part of the flaring disk behind it. This shadow can extend from the inner rim, at about 0.5 AU, out to 5 AU or more. Outward of this shadowing radius the disk adopts the usual flaring shape as described by CG97. This part of the disk is responsible for the observed emission at long wavelengths. Dependent on the height of the inner rim, the shadow can reach so far out that the 10 μm silicate emission feature, produced by warm dust in the surface layers, is suppressed. This has been used by DDN01 as a possible explanation for the lack of 10 micron feature in several sources.

Though succesful in explaining several features of the SEDs of Herbig Ae/Be stars, the DDN01 model was based on highly simplified equations. Among other things the structure of the inner rim and the shadowing of the disk behind it need closer theoretical examination. It is unclear from the DDN01 model what happens when the optical depth of the disk becomes too low to sustain flaring. Also, the DDN01 model was based on the assumption that, if the disk *can* flare outside the shadow, then it *will*. It is unclear whether perhaps in addition to these flaring disks also fully self-shadowed disk solutions exist.

Because of the intrinsic 2-D nature of the problem, a closer theoretical study requires a full 2-D treatment of radiative transfer. This is done with a 2-D "Variable Eddington Tensor" solver. By coupling the radiative transfer to the equations of vertical hydrostatic equilibrium, the code solves the entire temperature and density structure of the disk as a function of radius and vertical height above the midplane. As a simplifying assumption a grey opacity is adopted in this work. This is consistent with the disk consisting of large grains. The advantage of this simplification is that the results are more readily understood in terms of simple radiative transfer arguments. In a follow-up paper more realistic opacities and grain size distributions will be used, which will put us in a position to compare the results directly to observations.

Using the 2-D disk structure code just described, the following issues will be addressed:

1. Does the overall structure and SED of the disk agree with the much simpler model of DDN01? Will there indeed be a shadowed region behind the inner rim, as predicted by DDN01? How much will radial radiative diffusion heat this shadowed region, and how large is this region in radial direction?
2. Under which conditions will the outer part of the disk collapse into the shadow of the inner rim, making the disk entirely self-shadowed? Can there be a bimodal set of solutions (self-shadowed and flared) for the same parameters?
3. What is the structure of a fully self-shadowed disk? Will it be very cool and collapsed, or does radial radiative diffusion keep the disk still relatively warm?
4. What will the outer (tenuous) part of a large disk look like: will it continue to be flaring, or will it sink into the shadow of the flaring part of the disk?

The paper is organized as follows. In Sect. 2 the equations are presented, and it is described how they are solved. In Sect. 3 a model of a canonnical flaring disk around a Herbig Ae star is described, and in Sect. 4 it is shown that self-shadowed disk can exist and what their structure looks like. In Sect. 7 it is investigated if multiple solutions exist for the same parameters. A description of the tenuous outer parts of a flaring disk is given in Sect. 6.

2. The model equations

The model is based on 2-D radiative transfer to calculate the dust (and gas) temperature in the disk. Once the temperature is found it is then used to integrate the equations of hydrostatic equilibrium in order to find the density structure. The entire procedure is then iterated to obtain the full disk structure. Since the accretion rate in these disks is presumably very low, we do not include viscous dissipation in the equations.

The model equations and the computational method used in this work are quite similar to the ones used for the 1+1-D (vertical) structure models presented in Dullemond et al. (2002). However, here this method is extended to full 2-D. Details of this method will be presented elsewhere (Dullemond in prep.).

2.1. 2-D Radiative transfer

Consider a gas + dust density distribution $\rho(R,\Theta)$ as a function of the spherical coordinates R (radius) and Θ (angle as measured from the polar axis). A grey opacity $\kappa_\nu = \kappa$ is adopted, and the scattering albedo is assumed to be zero. The star is assumed to be a point source. The flux of direct starlight $F_*(R,\Theta)$ at every point in the disk is then given by:

$$F_*(R,\Theta) = \frac{L_*}{4\pi R^2}\exp(-\tau(R,\Theta))\,, \tag{1}$$

where $\tau(R,\Theta)$ is the optical depth in the radial direction between the point (R,Θ) and the central star, obeying the conditions:

$$\frac{\partial\tau(R,\Theta)}{\partial R} = \rho(R,\Theta)\kappa\,, \tag{2}$$

and $\tau(0,\Theta) = 0$. This direct stellar radiation is absorbed by the disk. The amount of energy per unit time and volume that is absorbed in this way is:

$$Q(R,\Theta) = \rho(R,\Theta)\kappa F_*(R,\Theta)\,. \tag{3}$$

By virtue of energy conservation this energy must then be reemitted as thermal (infrared) radiation by the dust in the disk. Dependent on the optical depth of the disk, this infrared radiation may be absorbed and re-emitted by the disk many times more, before it eventually escapes to infinity. It is this radiative diffusion process that allows the radiation to enter deep into the disk, and determine the temperature at every location, no matter at which optical depth.

To solve this complex 2-D radiative transfer problem, the re-emitted radiation field is treated as a separate radiation field, which will be called the "reprocessed radiation field" from now on. The dust grains acquire a temperature such that they emit exactly the same energy per second as they absorb:

$$\frac{\sigma}{\pi}\rho\kappa T^4 = \frac{Q}{4\pi} + \rho\kappa J\,, \tag{4}$$

where $J(R,\Theta)$ is the frequency-integrated mean intensity of the reprocessed radiation field. The mean intensity $J(R,\Theta)$ is defined as

$$J = \frac{1}{4\pi}\int_{4\pi} I(\Omega)\mathrm{d}\Omega\,, \tag{5}$$

where $I(\Omega)$ is the frequency-integrated intensity of the reprocessed radiation in the direction Ω. The first term in Eq. (4) accounts for the absorbed direct stellar radiation, while the second term takes into account the infrared radiation emitted by the disk itself.

The radiative transfer equation for the reprocessed radiation is:

$$\frac{\mathrm{d}I(\Omega)}{\mathrm{d}s} = \frac{\sigma}{\pi}\rho\kappa T^4 - \rho\kappa I(\Omega)\,, \tag{6}$$

which must be satisfied along every ray through the medium. Here s is the path length along the ray. The full 2-D radiative transfer problem amounts to solving the coupled set of Eqs. (4), (5), and (6). The formal transfer equation (Eq. (6)) has to be integrated along all rays through the disk. In practice this means that a discrete (but large) set of rays is chosen which samples the reprocessed radiation field as accurately as possible. The integration of Eq. (6) along all these rays is done using the method of "Extended Short Characteristics" (Dullemond & Turolla 2000).

Solving this set of equations is normally done using an iterative procedure from Eq. (6) to Eq. (5), to Eq. (4), and back to Eq. (6), until convergence is reached. This procedure is known as "Lambda Iteration" and is the basis of most current 2-D radiative transfer codes (including the original version of the program `RADICAL` described by Dullemond & Turolla 2000). However, at large optical depth this method leads to convergence problems since information about the radiation field propagates only one mean free path per iteration. This can be fatal for problems involving protoplanetary/protostellar disks. A rigorous solution to this problem is the "Variable Eddington Tensor" method, which couples the formal radiative transfer equation to the frequency-integrated moment equations (see e.g. Mihalas & Mihalas 1984; Malbet & Bertout 1991; Stone et al. 1992; Dullemond et al. 2002). `RADICAL` is now equipped with this method and can be used to solve 2-D radiative transfer problems at arbitrary optical depth with only a few iterations[1].

2.2. Vertical pressure balance

Once the temperature structure of the disk is determined, one can recompute the density structure by integrating the equations of vertical hydrostatic equilibrium:

$$\frac{\partial P}{\partial z} = -\rho\frac{GM_*}{R^3}z\,, \tag{7}$$

where z is defined here as $z = R(\pi/2-\Theta)$. Geometric correction factors are neglected in the above equation, i.e. it is assumed that the disk is still thin enough that these factors are unnecessary.

In order be able to solve Eq. (7), the surface density $\Sigma(R) = \int_{-\infty}^{\infty}\rho(R,z)\mathrm{d}z$ needs to be specified at every radius. For a given value of $\Sigma(R)$, the vertical density structure can be found by integrating Eq. (7) first for an initial guess of $\rho(z=0)$, and then renormalize it such that the required surface density is obtained. Having thus found the new density structure in this way, one can repeat the radiative transfer calculation for the next iteration step. Only when the new density structure is to within 10^{-2} of the previous density structure, this iteration procedure is terminated, and a solution is found.

The function $\Sigma(R)$ is an input to the problem, and is entirely free to choose. This reveils an intrinsic weakness of models of passive disks: since one is not constrained by a global (constant) accretion rate, one has no theoretical constraint on this input function. In principle this introduces an infinite number of degrees of freedom. In practice this problem is less severe. Disks are presumably formed with a relatively smooth surface density profile. And the SED of a passive disk depends only weakly on small scale variations in the surface density. As will be shown below, significant changes occur only if large parts of the disk switch from optically thick to optically thin or vice versa.

2.3. Determining the SED

Although the simplifying assumption of grey opacities is used in this paper, it is still useful to calculate the SED from the 2-D disk models. This is done by making images of the disk at a number of frequencies, and integrating these images to obtain the fluxes. The images are made using the ray-tracing capabilities of `RADICAL`. Care is taken that all spatial scales are sufficiently finely sampled.

Computing the SED at a large number of inclination angles allows for a very powerful self-consistency check of the radiative transfer solution: the total outcoming luminosity of the system should be equal to the luminosity of the star. At the end of each run `RADICAL` carries out such an energy conservation check. For all computed models, errors remained within 5% relative to the infrared luminosity of the disk.

[1] See web page `http://www.mpa-garching.mpg.de/PUBLICATIONS/DATA/radtrans/radical/`

3. A flaring disk around a Herbig Ae star

As a first step, the structure of a "typical" flaring disk around a Herbig Ae star is computed. As mentioned above, the surface density function $\Sigma(R)$ is a parameter of the model. It is given as a power law of the type:

$$\Sigma(R) = \Sigma_0 \, (R/\mathrm{AU})^p \tag{8}$$

where p is the power law index. Furthermore an inner radius $R_{\rm in}$ and an outer radius $R_{\rm out}$ is chosen, but it is verified that the inner radius $R_{\rm in}$ produces a dust temperature that is consistent with the 1500 K dust evaporation temperature for silicates. For most models this is at 0.7 AU, but for the optically thin model (model 3) a smaller inner radius is required. The parameters of the models are listed in Table 1. The one discussed in this section is model 1.

In Fig. 1 the temperature and density structure of the disk is shown. The disk is considerably cooler at the midplane than at its surface. This is because the matter deep within the disk is shielded from direct stellar light, and is only heated indirectly by the reprocessed radiation field. The inner rim, on the other hand, is directly exposed to the stellar radiation field, and is therefore much hotter than the rest of the disk. Directly behind the inner rim the temperature drops strongly, down to values much smaller than the optically thin dust temperature at the same radius.

Between 6 AU and the outer edge the disk adopts a typical flaring shape. The flaring of the disk can be recognized by following the kink in the temperature gradient. The relative height (z/R) of this kink increases with radius, showing that the surface height of the disk increases faster than R. This is the typical signature of flaring. This smooth temperature kink is the "surface layer" in which direct stellar radiation is absorbed and re-emitted as infrared radiation. Rather than a constant temperature (as in the simple model of Chiang & Goldreich and also DDN01), this surface layer has a temperature gradient going from the high temperatures of grains above the disk down to the lower temperatures of the grains deep within the disk.

The structure of the disk between the inner edge and about 6 AU is different from the usual flaring geometry. In the figure one sees that the vertical temperature gradient suddenly acquires a very steep jump at about $z/R \simeq \pi/2{-}\Theta = 0.18$. This is a result of the shadow of the inner rim. Below this line there is no direct stellar radiation, while above it a dust grain would be exposed to the full stellar flux. In the outer regions (beyond 6 AU) the surface of the disk lies above this shadow line, and therefore acquires the usual flaring disk shape. But at radii smaller than 6 AU the disk lies fully in the shadow, and is heated only by radial radiative diffusion. Note that, in the coordinate system used in Fig. 1, stellar radiation moves along horizontal lines from left to right.

The reason why the inner rim casts a shadow over the disk behind it is that the inner rim, being directly exposed to the stellar flux, is much hotter than the disk behind it, and consequently has a higher pressure scale height. This hot inner rim is therefore puffed up.

In Fig. 2 the same disk model was computed using the standard 1+1-D splitting, i.e. vertical plane-parallel radiative transfer (see e.g. Malbet et al. 1991; Dullemond et al. 2002). This model nicely reproduces the flaring shape of the disk. But it fails to reproduce the heating of the inner rim and the shadowed region. This shows that, while 1+1-D models can be used reasonably well to model disks at radii larger than several AU, they cannot be used for the inner regions.

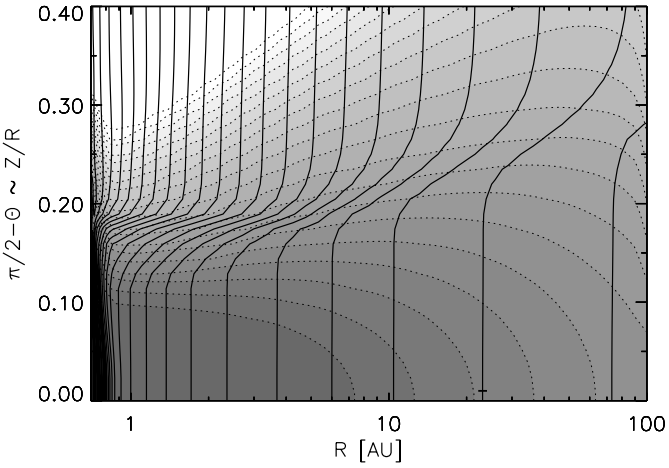

Fig. 1. The 2-D temperature and density structure of a flaring disk: model 1 discussed in Sect. 3. Contour lines represent the temperature and are spaced 50 K apart. A small "-" symbol marks the 100 K contour. Grey scales are density contours, logarithmically spaced such that 2 grey scale steps represent a factor of 10 in density. Dotted contours follow the grey scale contours, to aid the eye. The density contours are stopped at a gas density $\rho = 10^{-8}$ g/cm^3 to avoid color crowding. The horizontal axis is the (spherical) radius, in logarithmic scale. The vertical axis is the vertical height above the midplane measured in the angle $\pi/2{-}\Theta$, which is (to first approximation) equal to the vertical height z divided by the radius R. The equatorial plane is at the lower boundary of the figure. Note that in the coordinate system used here the stellar (primary) radiation moves along horizontal lines from left to right (i.e. at constant Θ). Therefore, the shadow cast by the inner rim can be recognized as a steep jump in the temperature along an exactly horizontal line in the figure (at $\pi/2{-}\Theta = 0.18$, ranging from the inner edge up to 6 AU).

Though the shadow is clearly seen in Fig. 1, in the shadowed region the midplane temperature does not drop very much. In fact, the temperature still increases as one goes towards smaller R. This shows that radial radiative diffusion manages to smear out radiative energy quite efficiently, so that even matter in the shadow of the inner rim (all the matter with $\pi/2{-}\Theta \lesssim 0.17$ in this case) will still be relatively warm, though colder than what it could be if the surface of the disk were out of the shadow. The thermal emission from this shadowed region is somewhat suppressed, as can be seen in Fig. 3. This suppression is less than what was expected by DDN01. This is because DDN01 used a very approximate formula to estimate the effect of radial radiative diffusion. In the present 2-D calculations the effect of this radial diffusion turns out to be stronger than predicted by DDN01.

From Fig. 3 it is also interesting to note that the emission per unit of $\log(R)$ is more or less constant for the flaring part of the disk (from about 3 AU onwards, up to shortly before the outer edge at 100 AU). Every radius of the flaring disk

Table 1. The parameters for the models in this paper. Columns 2, 3, 4 are the stellar parameters: mass in units of $M_\odot$, radius in units of $R_\odot$ and effective temperature in Kelvin. Column 5 is the vertical optical depth from $\Theta = 0$ to $\Theta = \pi$ at a radius of 1 AU. Column 6 is the radial optical depth at $\Theta = \pi/2$. Column 7 is the powerlaw index for the surface density such that $\tau_{\rm vert}(R) = \tau_{\rm vert}(1\ {\rm AU}) * (R/{\rm AU})^p$. Columns 8, 9 are the inner and outer radius of the disk in AU. Column 10 is for comments.

Model	$M_\star$	$R_\star$	$T_{\rm eff}$	$\tau_{\rm vert}$ (50AU)	$\tau_{\rm rad}$	p	$R_{\rm in}$	$R_{\rm out}$	Type
1	2.0	3.0	10 000	1.9×10^2	1×10^5	-1	0.7	100	Flaring
2	2.0	3.0	10 000	2.2	5×10^4	-2	0.7	100	Self-shadowed
3	2.0	3.0	10 000	7×10^{-4}	1	-1	0.3	100	Very tenuous disk
4	2.0	3.0	10 000	9.8	4×10^3	$-1, -2$	0.7	1000	Flaring + shadowed

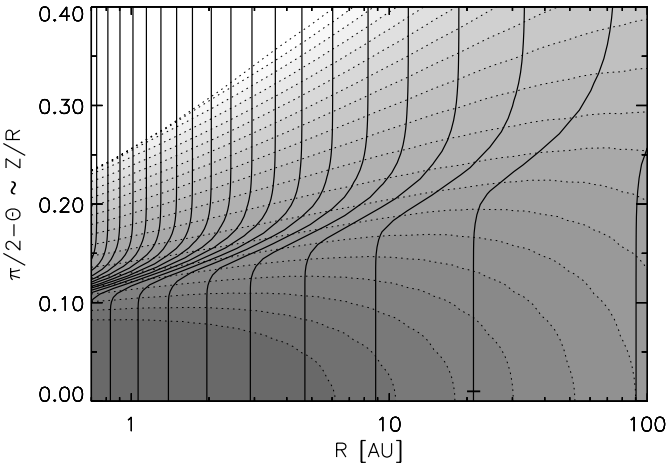

Fig. 2. Same as Fig. 1, but now computed using the standard 1+1-D approach to radiative transfer. It is clear that the effects of the hot inner rim and the shadowed region are not present using this 1+1-D approach.

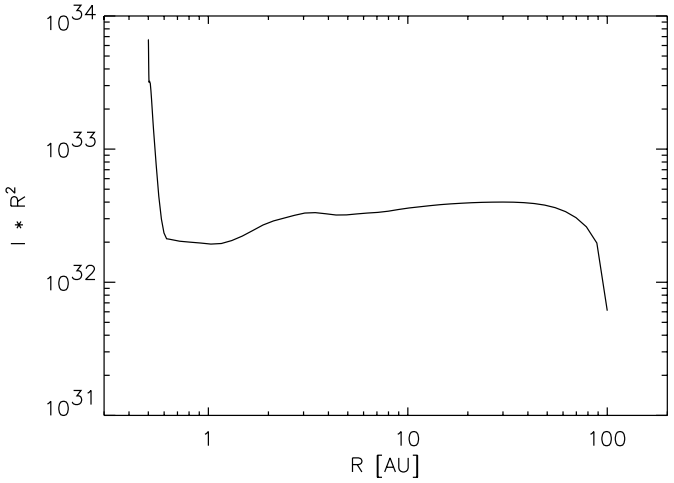

Fig. 3. The frequency-integrated intensity of the flaring disk (model 1) seen face-on, as a function of radius. This is computed by integrating the formal transfer integral (Eq. (6)) vertically through the disk. The multiplied by R^2 in order to weigh it with the emitting surface, so that it represents how strong the emission at each radius contributes to the SED. It is, so to say, the emission of the disk per constant interval in $\log(R)$.

constributes equally to the SED. This is a feature that can be understood in terms of geometry. The surface height $H_{\rm s}$ of the disk goes roughly as $H_{\rm s} \propto R^{9/7}$ (see CG97). This means that the flaring surface of the disk captures stellar luminosity in a way that is proportional to $R^{2/7}$. This is only a slowly varying function of R. In Sects. 4 and 6 two cases will be discussed where the flaring geometry of the disk breaks down. And indeed, it will turn out that the "equal emission per $\log(R)$" will also cease to hold. Note that at the very outer edge of the flaring disk the emission drops somewhat (Fig. 3). This is a result of radiative leaking of energy through the outer edge, and is therefore a 2-D radiative transfer effect.

In Fig. 4 the SED of the 2-D model is shown at various inclination angles. One can see that for face-on inclinations the 3-micron bump emission from the inner rim is very weak compared to the emission from the flaring part of the disk at longer wavelengths. This is because the inner rim is seen along the rim-surface, instead of perpendicular to it. At larger inclinations the inner rim emission gains in strength, while the flaring part fades. These are geometrical effects were predicted by DDN01 and seem to be confirmed here. It should be noted, however, that the strong supression of the near infrared bump at face-on inclinations is a result of the perfectly vertical inner rim that is assumed in our model. In reality, hydrodynamic effects will presumably make this inner rim more round (as in Fig. 12 below), which allows the near infrared emission to be seen also at face-on inclinations. As there is observational evidence that even face-on disk show considerable near-infrared emission (e.g. Millan-Gabet et al. 1999), it is important to investigate such hydrodynamic "smoothing" of the inner rim in more detail in the near future.

Images of how the disk actually looks like when viewed at a certain inclination angle are shown in Fig. 5 in logarithmic grey scale. A wavelength of 50 μm is chosen so that the entire disk radiates sufficiently brightly. In the upper-left image one sees the outer edge of the disk. It is evident that the surface layers radiate strongly, while the midplane layers are dimmer. As one zooms in, the intensity of the disk's surface gets stronger, and finally the bright inner rim appears. The inner rim is much brighter than the rest of the disk, as can be seen in linear grey scale (the lower-right image). The far side of the rim provides most of the flux. The inner rim therefore appears as an ellipse with one side brighter than the other. This asymmetry will presumably be less strong if one takes into account the smoothing of the inner rim by hydrodynamic effects, as discussed above. A strong shadowed region does not show up clearly in these images, dispite the fact that the shadow is indeed there (see

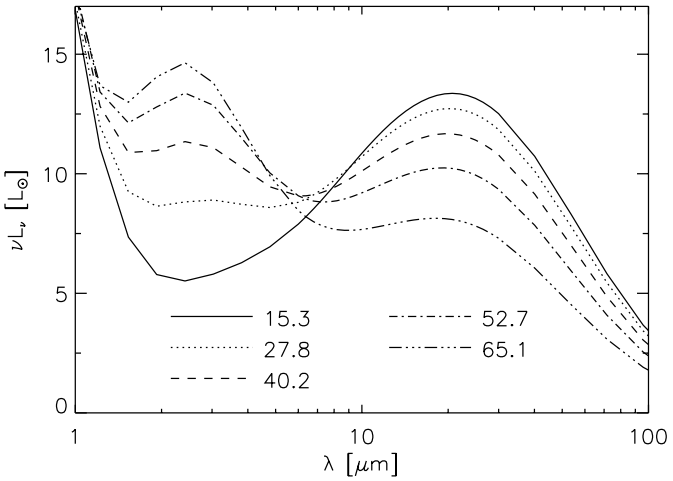

Fig. 4. The spectral energy distribution (for grey opacities) for model 1, computed at different inclination angles. The stellar atmosphere is included, but is approximated by a blackbody for simplicity. The inclination angles are measure from the pole (i.e. $i = 0$ means face-on). Note that the vertical scale is linear.

Figs. 1 and 3). Clearly the radial radiative diffusion prevents the shadowed region from becoming too cold.

4. Self-shadowed disks

For disks that do not reach a certain minimal mass, it can happen that the entire disk will sink into the shadow of the inner rim. At no point the vertical optical depth is then large enough that the surface of the disk reaches out of the shadow. The disk (apart from the inner rim) is therefore not directly heated by the stellar radiation, and will therefore cool down. Since the temperature determines the vertical height, the disk will therefore shrink even deeper into the shadow. The temperature and density structure of such a disk is shown in Fig. 6. The shadow is now clearly seen to extend all the way towards the outer edge of the disk. Yet, the self-shadowed disk is not entirely cold, as can be more clearly seen in Fig. 7. Although no part of the disk behind the inner rim can see the star directly, there is still sufficient indirect heating by the reprocessed radiation of the inner parts of the disk, and by radial radiative diffusion, that the self-shadowed disk remains relatively warm.

The self shadowed disk has no hot surface layer: the temperature is more or less the same at every height above the midplane. Only at elevations significantly above the photosphere of the disk, where one gets in direct sight of the star, does the temperature rise to the optically thin dust temperature. But at those elevations the densities are already so low that one cannot speak of a hot surface layer anymore.

In Fig. 8 the SED of the self-shadowed disk is shown, and compared to the SED of a flaring disk. Although this SED has been computed here only for grey opacities, it is interesting to note that the SED of the self-shadowed disk has a much steeper slope towards long wavelengths ($\nu F_\nu \propto \nu^{1.1}$) than the flared disk ($\nu F_\nu \propto \nu^{0.2}$), which is a result of the steeper temperature slope of these disks. One may speculate whether such self-shadowed disks may be the explanation for the group II

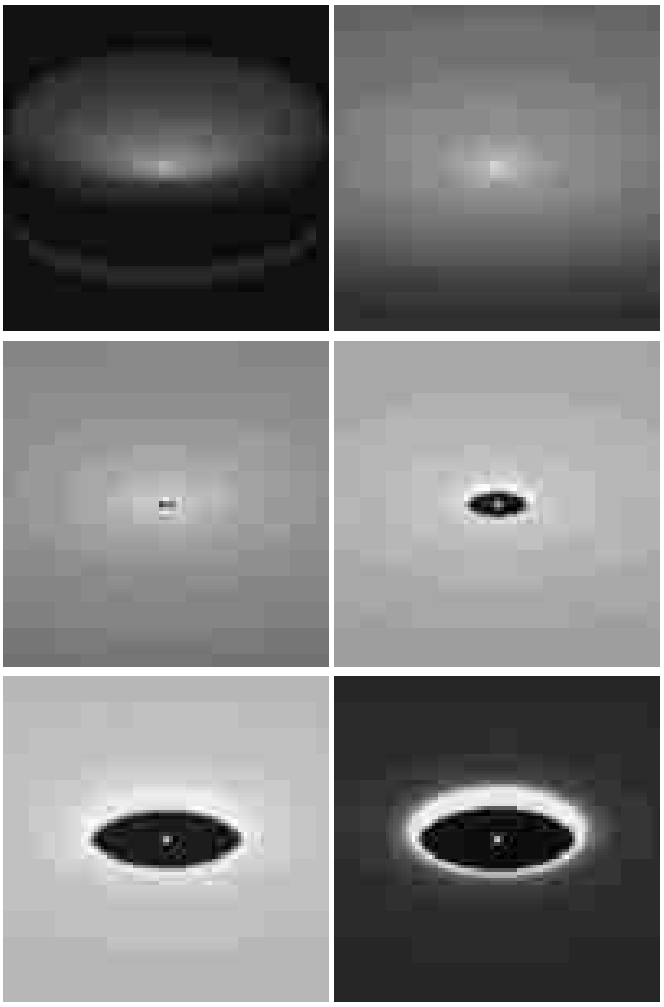

Fig. 5. Images of the flaring disk (model 1) at varying zoom factor. All images, with the exception of the bottom-right image, are in logarithmic grey scale. The bottom-right image is the same as the bottom-left image, but then in linear grey scale. From top-left to bottom-right the images show the entire disk, zoomed in to the bright inner rim. The images are taken at 50 μm.

Herbig Ae/Be stars in the classification of Meeus et al. (2001). These sources show a weak far infrared emission, and have an overall SED shape very similar to the SED computed here for the self-shadowed disks. Moreover, the similar strength in the near-IR emission between self-shadowed and flared disks is also observed between group I and group II sources. Yet, these group II sources have strong silicate emission features, which might not be consistent with such self-shadowed disks. Also, mm observations indicate that group II sources are still quite massive, and it remains to be proven whether these disks are not too massive to be self-shadowed. To answer these questions, a similar disk model, but with more realistic dust opacities must be carried out. This will be one of the subjects of a follow-up paper (Dullemond & Dominik in prep.).

5. Very tenuous disks

When the optical depth measured along the equatorial plane becomes smaller than unity, the height of the shadow drops

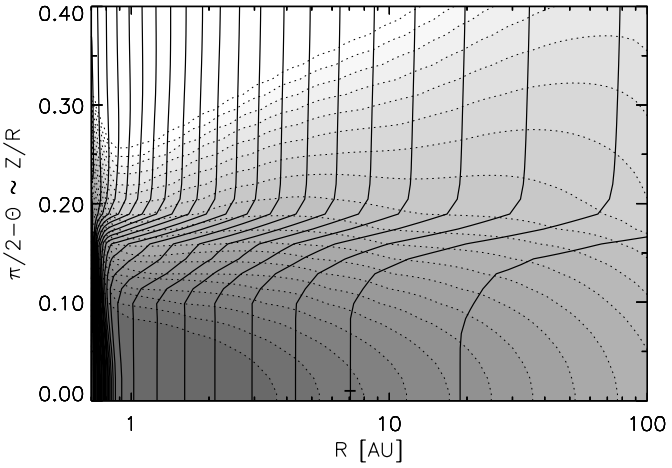

Fig. 6. The temperature and density structure of a self-shadowed disk: model 2 discussed in Sect. 4. Contour lines represent the temperature and are spaced 50 K apart. A small "-" symbol marks the 100 K contour. Grey scales are density contours, logarithmically spaced such that 2 grey scale steps represent a factor of 10 in density.

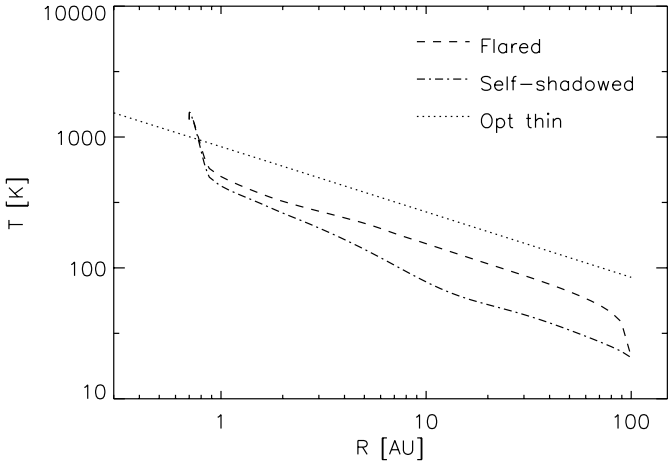

Fig. 7. The temperature at the equator as a function of R, for the self-shadowed disk of model 2 (dot-dashed line) and for the more massive flaring disk of model 1 (dashed line). The temperature for a completely optically thin configuration is shown as a dotted line. Note that the temperature of models 1 and 2 near the inner edge (0.7 AU) exceeds the optically thin dust temperature. This is a backwarming effect by the optically thick inner rim.

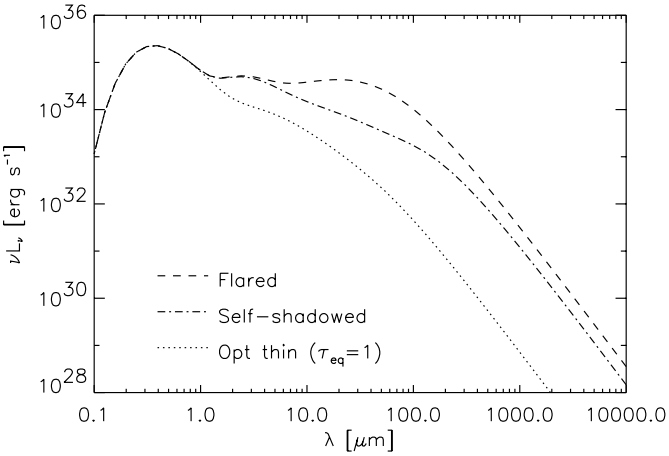

Fig. 8. The spectral energy distribution of the flaring disk of model 1 (dashed line), the self-shadowed disk of model 2 (dot-dashed line), and the optically thin disk of model 3 (dotted line).

to zero and the disk becomes unshadowed again. In this case not only the vertical optical depth $\tau_{\rm vert}$ is smaller than unity, but the optical depth along any ray through the disk is smaller than one. It can be considered as a fully optically thin disk. Since such a disk has no surface layer which captures the stellar radiation (as in model 1), the disk is not a "flaring disk" as such. Yet, the density structure is still "flared" in another sense: the dimensionless pressure scale height $h_{\rm p} \equiv H_{\rm p}/R$ increases outwards, as can be clearly seen from the density contours in Fig. 9. This is easily understood, since the temperature of a grey dust grain goes as $T \propto 1/\sqrt{R}$ and the pressure scale height scales as $H_{\rm p} \propto \sqrt{TR^3}$, giving $H_{\rm p}/R \propto R^{1/4}$.

Model 3 is a model with an equatorial optical depth (radial optical depth along the midplane) of $\tau_{\rm rad} = 1$. In Fig. 9 the temperature and density structure of this disk is shown. It is clear that the temperature is only modestly influenced by the extinction at the equator, and that the overall density structure is that of a purely optically thin disk. The covering fraction of this disk is very small, and therefore the infrared excess of this disk is small compared to the stellar flux (Fig. 8).

The optically thin model presented here (model 3) may not be very realistic. In such very tenuous disks the temperature of the dust and the gas may start to decouple. Gas heating/cooling, dust-gas thermal energy exchange and dust drift should then be properly taken into account (see e.g. Kamp & van Zadelhoff 2001).

6. Outer regions of flaring disks

Generally it is assumed that the surface density $\Sigma(R)$ of a protoplanetary disk decreases as a function of radius. It can happen that a disk of the usual "rim + shadow + flaring" type will become too optically thin in the outer parts to maintain flaring beyond a certain radius $R_{\rm turn}$. The $\tau_V = 1$ surface, where the stellar radiation is captured by the disk, in effect turns over and no longer maintains the necessary flaring shape necessary to capture stellar radiation. The hot surface layer ceases to exist beyond that radius. The outer regions can now only be heated indirectly by the infrared radiation of the disk itself. This prevents the disk from collapsing to zero scale height.

Model 4 is a model that has such a non-flaring outer part. To aggravate the situation so that the results are more clear, the surface density distribution is taken to be a broken powerlaw ($p = -1$ inwards of 50 AU an $p = -2$ outwards of 50 AU). But the self-shadowed outer regions can occur also for single-powerlaw surface density slopes, though the dimming of the emissivity is then weaker.

In Fig. 10 the temperature structure of this disk is shown. The shadowing effect is not very clear from the solid contours. That is why a number of finer-spaced contours are added in the figure (dashed lines). The shadow is apparent in the same way as it was for the shadow of the inner rim: a horizontally arranged temperature jump. But a better way to see the effect of

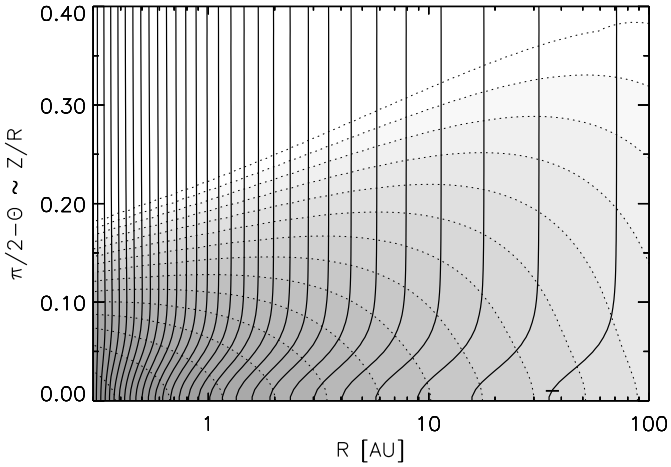

Fig. 9. The temperature and density structure of an almost optically thin disk: model 3 discussed in Sect. 5. Contour lines represent the temperature and are spaced 50 K apart. A small "-" symbol marks the 100 K contour. Grey scales are density contours, logarithmically spaced such that 2 grey scale steps represent a factor of 10 in density.

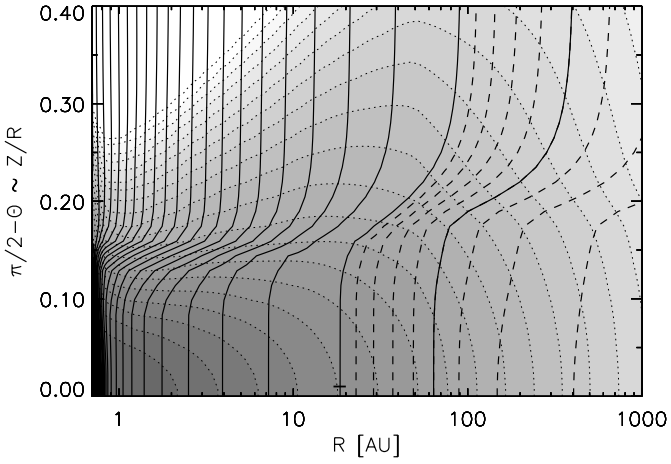

Fig. 10. The temperature structure of a large disk which becomes optically thin to stellar radiation at the outer parts: model 4 discussed in Sect. 6. Contours are 50 K apart. A small "-" symbol marks the 95 K contour. The dashed lines are also temperature contours, but with a spacing of 5 K, in order to make the structure at large radii more clear. Note that the radial range is larger than in the previous figures of this kind.

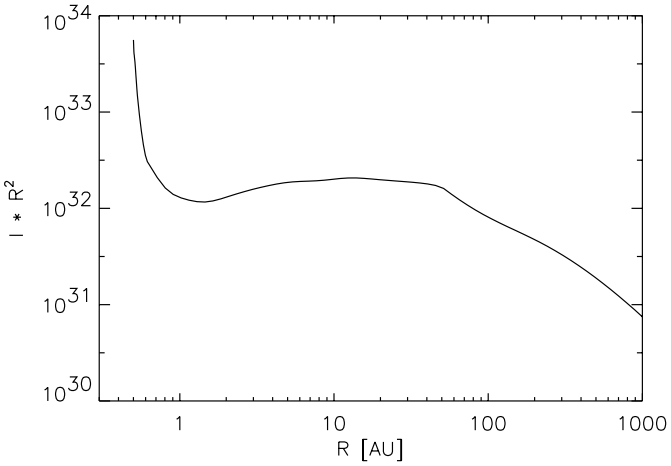

Fig. 11. As Fig. 3, but now for model 4.

the shadowing of the outer regions is to compute the emission of the disk per $\log(R)$, as shown in Fig. 11. It is clearly seen that the continuum emission drops strongly in the shadowed outer regions, and will therefore only make a small contribution to the SED.

This result may go some way towards explaining the differences that are often encountered when measuring the radius from SED fitting, mm continuum interferometric mapping and CO line interferometric mapping (e.g. Mannings et al. 1997; Mannings & Sargent 1997; Dominik et al. 2002). As the results of this model show, all of the radiation of the star is reprocessed within $R_{\rm turn}$, since the disk is incapable of capturing radiation beyond that radius. So the SED will be dominated by the disk structure within $R_{\rm turn}$, and the emission from the outer parts will be weak in comparison. Therefore the outer radius as inferred from SED fitting will yield $R_{\rm out} = R_{\rm turn}$. But in interferometric maps one can see also the region beyond $R_{\rm turn}$, even though it is much dimmer than the emission from the flaring parts of the disk. CO rotational lines, since they are density tracers, will be less senstive to this temperature drop. They may even be more easily detected in these outer regions, which may yield even larger effective disk sizes, unless CO is strongly depleted by freezing out onto dust grains.

7. Bimodal solutions?

In the paper of DDN01 the possibility was raised that two disk solutions might exist for the same disk parameters, namely one where the disk has the rim+shadowed region + flaring part structure, discussed in Sect. 3, and one where, on the contrary, the whole disk is in the shadow of the inner rim, as discussed in Sect. 4. This is an important point because, if proven, it would mean that the actual shape of a disk depends not only on its properties such as mass and radius, but also on its previous evolution.

The reasoning is as follows. Suppose we do not consider the process of radial radiative transport, and assume that the interior of the disk is only heated by radiation from the surface layer that diffuses downwards, but not sideways to other radial shells. In such a scenario it is unclear why the disk should always flare (and pop out of the shadow) at radii where it can. Suppose we could artifically cool the flaring part of the disk down for a moment. Then the disk will shrink in height and retreat back into the shadow. Once in the shadow, it won't receive radiation from the star (the surface remains below the shadow line), and therefore the disk remains cool and stays in the shadow. Hence we would have found a second solution. In the DDN01 paper it was argued that presumably nature will pick the flaring solution only. Yet this remained to be proven.

With the 2-D radiative transfer code one is now in a position to do this, since 2-D transfer automatically includes the effect of radial radiative diffusion and indirect heating by radiation from the inner regions. The parameters of the disk are chosen such that it is only marginally flaring. The iteration of the disk structure computation was started from two different

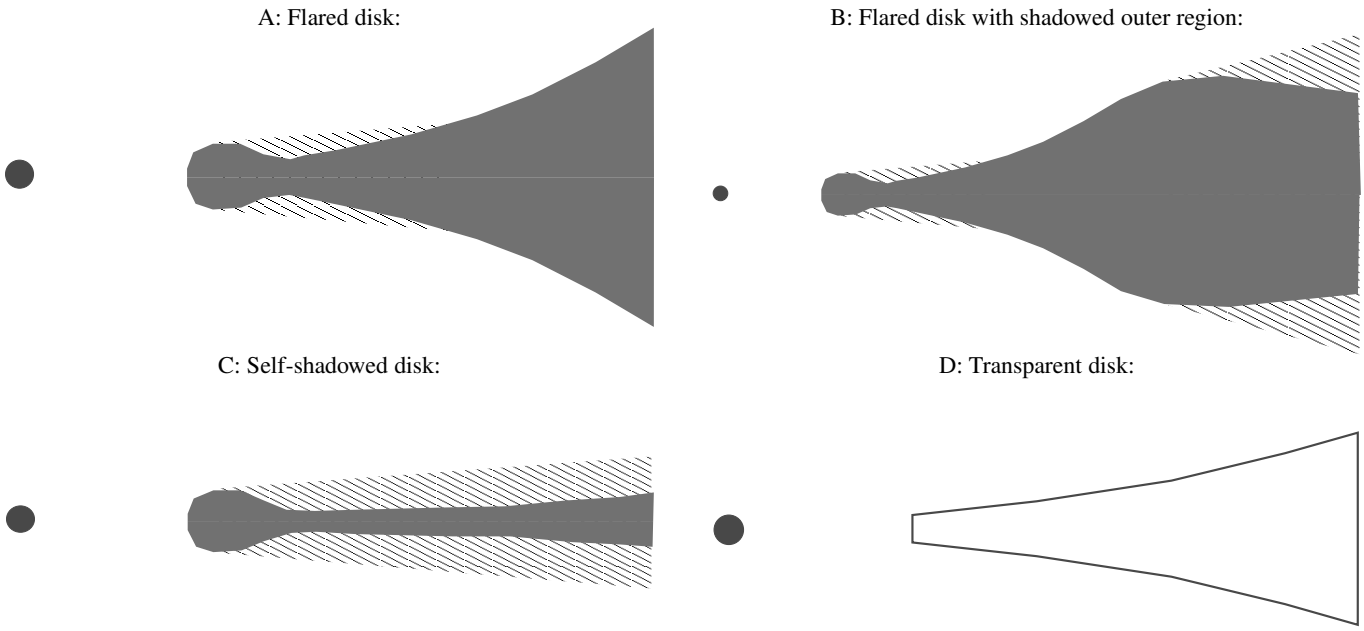

Fig. 12. Pictograms showing the four main kinds of solutions found. They represent a vertical cross-section of the disk, but are not to scale. A hashed area represents a shadow. In cases A, B and C the vertical optical depth may, under some conditions, drop below zero even though the radial optical depth remains much larger than unity. Case B is "zoomed out" to indicate that the second shadowing happens at large radii. In case D, the empty polygon is meant to show that even the radial optical depth along the midplane is small, meaning that the temperature everywhere is set by the optically thin dust temperature. The cases A, B, C and D are ordered according to decreasing optical depth (i.e. mass of the disk). It should be noted, however, that such an ordering does not always strictly apply since the powelaw index p of the surface density distribution also plays a role in determining the disk shape.

initial guesses for the vertical pressure scale height. One was a normal flaring disk ($H_{\rm p} \propto R^{2/7}$), and one was a fully self shadowed disk ($H_{\rm p} \propto R^{-2/7}$).

It was found that both initial guesses reach the same solution, which is a "rim + shadow + flaring" disk. This procedure was tried for a series of parameters and optical depths. In each case only a single solution was found. This means that the possibility of bimodal solutions seems to be excluded, at least within the present assumption of grey opacities. The conclusion is what one could call the "flaring disk principle": a disk will flare whenever and wherever it can. Only if the disk cannot flare, because of too low optical depth, then it will remain self-shadowed.

The question of bimodal solutions is also loosely linked to the question of stability. Based on a time-dependent version of the equations of CG97 for an irradiated flaring disk it can be shown that such disks should be unstable to self-shadowing (Dullemond 2000; Chiang 2000). Such disks would quickly develop ripples on the surface, which eventually cause most of the disk to collapse. However, these conclusions were based entirely on the highly simplified equations of CG97. It appears that 2-D radiative transfer effects will stabilize the disk (Dullemond in prep.). The radial thermal coupling between neighboring parts of the disk prevents the development of strong temperature gradients.

8. Conclusions

In this paper the structure of passive circumstellar disks was theoretically investigated. The problem was defined in a mathematically "clean" way: it is the problem of computing the temperature and density structure of rotating circumstellar matter around a star with a certain mass, radius and luminosity from basic principles of radiative transfer, radiative equilibrium and vertical hydrostatic equilibrium. The disk parameters that went into the calculation were the inner and outer radius, and the surface density distribution as a function of radius. The only mathematical approximation made here was the reduction of the hydrostatic equilibrium equations to 1-D vertical equations. From a physical point of view, many more approximations were made (related to dust-gas coupling, active accretion, dust opacities, etc.). But these were necessary to keep the problem clear of uncertain physics for now.

Four different kinds of solutions were found: a flaring disk, a self-shadowed disk, a transparent disk, and a flaring disk with self-shadowed outer region. These solutions are pictographically listed in Fig. 12. The numerical models described in this paper can be downloaded from a website: `www.mpa-garching.mpg.de/PUBLICATIONS/DATA/radtrans/grey2d/`.

The main conclusions are summarized as follows:

1. A flaring disk around a Herbig Ae/Be star has a hot inner rim, a shadowed region behind it, and the usual flared geometry at large radii (Fig. 12A). These findings are in accordance with the predictions of Dullemond et al. (2001). But the effect of shadowing in suppressing the emission from the shadowed region is not as strong as was predicted in that paper.
2. Disks with intermediate to low vertical optical depth but high equatorial optical depth can become entirely self-shadowed (Fig. 12C). The SED falls off more steeply at long wavelength than for flaring disks.
3. Disks with equatorial optical depths that are smaller than unity are un-shadowed again, since the inner rim can no longer stop the stellar radiation. These disks are fully optically thin (Fig. 12D).
4. The outer regions of flared disks can become shadowed if beyond a certain radius the surface density becomes too low. This time it is the flared part of the disk that casts the shadow (Fig. 12B). These outer parts do not contribute much to the SED, but may still be detectable using (sub-)millimeter interferometers. Measurements of the outer radius of a disk may therefore yield different results, depending on whether one uses SED-fitting, continuum mapping or CO mapping.
5. In the case of self-shadowed disks, and the shadowed outer parts of flaring disks, the usual 1+1-D approach to disk modeling breaks down, and so does the approach used by CG97 and DDN01. A full 2-D approach, such as the one used in this paper, is then necessary. It might be that the SED is still relatively well described using a 1+1-D model or a DDN01-type model up to the self-shadowing radius, but this remains to be proven using a 2-D model with more realistic opacities.
6. Bimodel solutions were not found. It seems that protoplanetary disks obey a kind of "flaring disk principle": if the disk *can* flare, it *will*. Self-shadowed disks are therefore disks which cannot be made to flare.

Many of these conclusions will presumably still hold when more realistic opacities are included. But this will be the topic of the second paper in this series.

Acknowledgements. I wish to thank Carsten Dominik and Antonella Natta for their careful reading of the manuscript and many interesting remarks, Tom Abel for inspiring me during the debugging of the variable eddington tensor code, and Rens Waters and G.-J. van Zadelhoff for useful discussions. I acknowledge support from the European Commission under TMR grant ERBFMRX-CT98-0195 ("Accretion onto black holes, compact objects and prototars").

References

Augereau, J. C., Lagrange, A. M., Mouillet, D., & Ménard, F. 2001, A&A, 365, 78
Chiang, E. 2000, Ph.D. Thesis, California Institute of Technology
Chiang, E. I., & Goldreich, P. 1997, ApJ, 490, 368
D'Alessio, P., Calvet, N., Hartmann, L., Lizano, S., & Cantó, J. 1999, ApJ, 527, 893
D'Alessio, P., Canto, J., Calvet, N., & Lizano, S. 1998, ApJ, 500, 411
di Francesco, J., Evans, N. J., Harvey, P. M., Mundy, L. G., & Butner, H. M. 1994, ApJ, 432, 710
Dominik, C., Dullemond, C., Waters, L., & Walch, S. 2002, A&A, submitted
Dullemond, C. P. 2000, A&A, 361, L17
Dullemond, C. P., Dominik, C., & Natta, A. 2001, ApJ, 560, 957
Dullemond, C. P., & Turolla, R. 2000, A&A, 360, 1187
Dullemond, C. P., van Zadelhoff, G. J., & Natta, A. 2002, A&A, 389, 464
Grady, C. A., Woodgate, B., Bruhweiler, F. C., et al. 1999, ApJ, 523, L151
Grinin, V. P., & Rostopchina, A. N. 1996, Ann. Rep., 40, 171
Hillenbrand, L. A., Strom, S. E., Vrba, F. J., & Keene, J. 1992, ApJ, 397, 613
Kamp, I., & van Zadelhoff, G.-J. 2001, A&A, 373, 641
Malbet, F., & Bertout, C. 1991, ApJ, 383, 814
Mannings, V., Koerner, D. W., & Sargent, A. I. 1997, Nature, 388, 555
Mannings, V., & Sargent, A. I. 1997, ApJ, 490, 792
Meeus, G., Waters, L. B. F. M., Bouwman, J., et al. 2001, A&A, 365, 476
Mihalas, D., & Mihalas, B. 1984, Foundations of radiation hydrodynamics (Oxford University Press)
Millan-Gabet, R., Schloerb, F. P., & Traub, W. A. 2001, ApJ, 546, 358
Millan-Gabet, R., Schloerb, F. P., Traub, W. A., et al. 1999, ApJ, 513, L131
Miroshnichenko, A., Ivezić, Z., Vinković, D., & Elitzur, M. 1999, ApJ, 520, L115
Miroshnichenko, A., Ivezic, Z., & Elitzur, M. 1997, ApJ, 475, L41
Natta, A., Prusti, T., Neri, R., Wooden, D., & Grinin, V. P. 2001, A&A, 371, 186
Palla, F., & Stahler, S. W. 1993, ApJ, 418, 414
Pezzuto, S., Strafella, F., & Lorenzetti, D. 1997, ApJ, 485, 290
Qi, C. 2001, Ph.D. Thesis, California Institute of Technology
Stone, J., Mihalas, D., & Norman, M. 1992, ApJS, 80, 819
Strom, S. E., Strom, K. M., Yost, J., Carrasco, L., & Grasdalen, G. 1972, ApJ, 173, 353
Tuthill, P. G., Monnier, J. D., & Danchi, W. C. 2001, Nature, 409, 1012
van den Ancker, M. E., Bouwman, J., Wesselius, P. R., et al. 2000, A&A, 357, 325
van den Ancker, M. E., de Winter, D., & Tjin A Djie, H. R. E. 1998, A&A, 330, 145
Vink, J. S., Drew, J. E., Harries, T. J., & Oudmaijer, R. D. 2003, A&A, submitted